2

Materials synthesis and characterizations

2.1 Introduction

This chapter describes the synthesis of materials and characterization tools used for their analysis. The nanocomposites of C with pure Fe_3C or pure Fe_3C/Fe_3O_4 or $Zn_xFe_{3-x}C$ or Mn or Ni substituted (Fe_3C/Fe_3O_4) were synthesized by sol-gel assisted technique. The phase identification and their structural properties were analyzed with the help of X-ray diffraction (XRD). Transmission electron microscope (TEM) was used to determine the morphology and size distribution of the nanoparticles. The colloidal stability of the nanoparticle in aqueous media was evaluated by Zeta potential. Fourier transform infrared spectroscopy (FTIR) validates the adsorbed molecules of the surfactants over the nanoparticles during the functionalization process. The oxidation states of the element present in the samples were analyzed by X-ray photoelectron spectroscopy (XPS). Further, Mossbauer spectroscopy was carried out to identify the phases in the nanoparticles. The magnetic properties of the samples were investigated using magnetic properties measurement system (MPMS). Magnetic hyperthermia experiment were accomplished for the evaluation of the heating efficacy of magnetic ferrofluids. The cytotoxicity assessment of these pure and substituted nanoparticles were examined using Sulforhodamine B assay (SRB). Fluorescence microscopy was carried out to observe the alteration in the morphology

(physical, chemical and mechanical damages) of the cells treated with ferrofluids for a certain period. Further, these nanocomposites were employed for the photocatalytic activities evaluation and electrochemical performance as anode in LIB_S.

2.2 Materials

All the precursors were purchased from the Merk (≥ 99.9% purity) and used directly without any further purification. The precursors used for synthesis of the samples were anhydrous $FeCl_3$, $ZnCl_2.xH_2O$, $NiCl_2.6H_2O$, $MnCl_2.6H_2O$, urea, CTAB and ethanol as a solvent.

2.3 Synthesis Method

As discussed in the Chapter-1, there are numerous techniques reported in the literature to get the Fe_3C phase. However, the present study deals with sol-gel assisted route followed by calcination at 700 ℃ in N_2 atmosphere. The sol-gel process involves four stages: (a) hydrolysis: formation of stable dispersion of colloidal particles in a solvent i.e. "sol" (b) condensation/polymerization of monomers: 3 D continuous network by joining polymer chains (c) growth of particles: formed aggregates due to interactions between the sol' particles and (d) gel formation: covalent-type interactions dominate and transformed to gel. In addition, these processes can be influenced by several parameters such as pH, temperature, concentration of the reactants, and the additives.

For the preparation of Fe_3C MNP_S, initially, iron (III) chloride anhydrous (3 g), urea (18 g) powder in 1: 6 ratio, as well as CTAB (2 g) were added into the solution of ethanol and distilled water (DW) (40 ml each). The solution was heated at 70 °C till it gets transformed into a light-yellow gel. The resulting gel was then

kept inside an oven at ~200 °C. This transformed the gel into a foam-like solid. Afterward, the sample was heat treated at 700 °C in a nitrogen atmosphere for 3 h. The obtained black color powder was washed with 30 % of H_2O_2 solution in water to remove the excess carbon. Furthermore, the probe sonicator and high-frequency ultrasonicator were employed for half an hour to reduce the size of the particles.

Similarly, the nanocomposite $Fe_3C/Fe_3O_4/C$ was prepared by this technique, as mentioned earlier. However to obtain oxide phase the N_2 gas flow was stopped after calcination at 700 ºC i.e. the sample was cooled to room temperature in air. Likewise, Ni or Mn-substituted nanocomposites were synthesized under similar circumstances using the stoichiometric amount $NiCl_2.6H_2O$ or $MnCl_2.6H_2O$ along with anhydrous $FeCl_3$ as precursors. The schematic diagram for the synthesis of nanoparticles is shown in Fig. 2.1. The nomenclatures for the Ni-substituted and Mn-substituted nanocomposites are listed in the Tables 2.1 and 2.2 respectively.

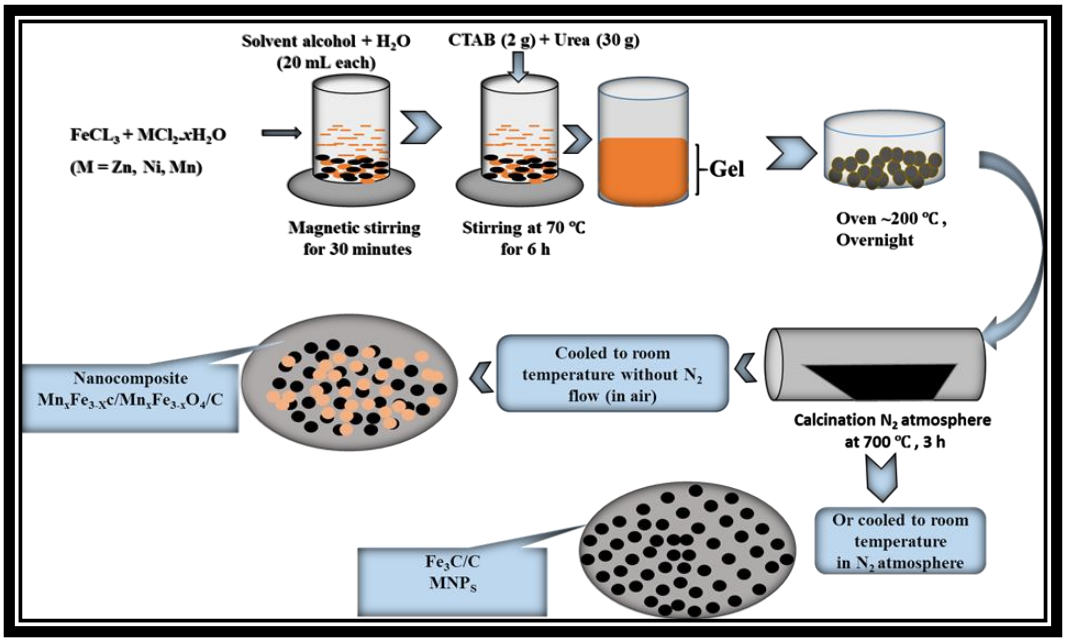

Figure 2.1: Schematic representation of synthesis protocol for the nanocomposites.

Table 2.1: Nomenclature of the pure and unsubstituted as well as Ni substituted (Fe_3C/Fe_3O_4)/C nanocomposites:

Sr no.	Samples	Phases	Precursors	Substitution
1	FC	Fe_3C/C	$FeCl_3$, urea, CTAB	Without Ni substituted samples
2	FOC	Fe_3C/Fe_3O_4/C	$FeCl_3$, urea, CTAB	
3	N1FOC (x = 0.1)	$Ni_aFe_{3-a}C/Ni_bFe_{3-b}O_4$/C	$NiCl_2{\cdot}6H_2O$, $FeCl_3$, Urea, CTAB	Ni substituted samples
4	N3FOC (x = 0.3)	$Ni_cFe_{3-c}C/Ni_dFe_{3-d}O_4$/C	$NiCl_2{\cdot}6H_2O$, $FeCl_3$, Urea, CTAB	
5	N5FOC (x = 0.5)	$Ni_eFe_{3-e}C/Ni_fFe_{3-f}O_4$/C	$NiCl_2{\cdot}6H_2O$, $FeCl_3$, Urea, CTAB	

Note: The terms a and b or c and d or e and f indicate the values of Ni in Fe_3C and Fe_3O_4 phases for x = 0.1, 0.3 and 0.5 samples i.e. a + b = 0.1, c + d = 0.3 and e +f = 0.5. Nevertheless, it is quite tricky to get exact values for a, b, c, d, e and f.

Table 2.2: The nomenclature for the Mn-Substituted (Fe_3C/Fe_3O_4)/C nanocomposites.

Sr. no.	Samples	Phases	Precursors	Substitution
1	FC	Fe_3C/C	$FeCl_3$, urea, CTAB	Without Mn substituted
2	M2FOC (x = 0.2)	$Mn_pFe_{3-p}C/Mn_qFe_{3-q}O_4$/C	$MnCl_2{\cdot}6H_2O$, $FeCl_3$, Urea, CTAB	Mn substituted samples
3	M7FOC (x = 0.7)	$Mn_rFe_{3-r}C/Mn_sFe_{3-s}O_4$/C	$MnCl_2{\cdot}6H_2O$, $FeCl_3$, Urea, CTAB	

Note: The terms p and q or r and s indicate the values of Mn in Fe_3C and Fe_3O_4 phases for x = 0.2 and 0.7 samples i.e. p + q = 0.2, and r + s = 0.7. Nevertheless, it is quite tricky to get exact values for p, q, r, and s.

2.4 Characterization Techniques

2.4.1 X-ray diffraction

All the X-ray diffraction patterns were obtained with Cu K_α radiation (λ = 1.54056 Å) by an X-ray powder diffractometer (BT- Rigaku Miniflex) in the range of 25 to 90° for analysis of the obtained phase and structure. The applied voltage and current were 40 kV and 200 mA respectively. The X-ray diffraction peaks for the samples were fitted with Voigt function. The corresponding Lorentzian and Gaussian

component were utilized for the estimation of crystallite size. The crystallite size was calculated using Scherrer's equation [119]:

$$t = 0.91\lambda/\beta_L \cos\theta \quad \text{.....2.1}$$

where t is the average crystallite size, λ is the wavelength of incident radiation (Cu K_α radiation), θ is Bragg angle. The term β_L is full width at half maximum in radians ($\beta_L = \beta_{exp.} - \beta_I$), $\beta_{exp.}$ is obtained full width at half maximum of the sample (Lorentzian component) and β_I is instrumental broadening which was measured using standard silicon sample.

2.4.2 Transmission Electron Microscopy (TEM)

The morphology and size of the particles were observed using transmission electron microscopes (TEM, PHILIPS CM 200 and TEM, TECNAI-20 G^2) operating at an accelerating voltage of 200 kV. For the sample preparation, small amount of the powder was dispersed into methanol and ultrasonicated for few minutes at room temperature. Then, single drop of the suspension was put on the carbon coated copper grid and dried for few hours in front of infrared lamp (IR lamp) before observing under TEM. The selected area electron diffraction (SAED) pattern was recorded to detect the phases present in the sample.

2.4.3 Colloidal stability

Zeta sizer (Malvern Instruments) was used to analyze the colloidal stability of pluronic F-127 functionalized nanoparticles in aqueous medium at ambient conditions after homogenization. The experiment was carried out for thrice at each pH value (ranging from acidic to basic region, 1 - 12). The instrument was calibrated using a latex suspension of known zeta potential (i.e., ± 55 to ± 5 mV).

2.4.4 X-ray photoelectron spectroscopy

The surface of the sample was analyzed by X-ray photoelectron spectroscopy (XPS) of PHI5000 Versaprobe II photoelectron spectrometer (ULVAC-PHI) to determine the elements present and their respective oxidation states. Al Kα X-ray beam (1486.61 eV) having dual anode was used as the source. Shirley background function was used for baseline correction.

2.4.5 Mössbauer spectroscopy

Mössbauer spectrum was logged in standard transmission geometry in the stable acceleration mode or triangular waveform. The ^{57}Co in Rh matrix at room temperature was used as a source. An α-Fe was used as a standard to calibrate the spectrometer. Isomer shift values were estimated relative to it. The experimental data were fitted using the least square curve fitting model.

2.4.6 Magnetic properties measurement system

Magnetic measurements were performed on SQUID (MPMS-XL, Quantum Design). The powder sample were loaded into standard Teflon tubes and magnetic data were collected up to the applied field of ±2 T.

2.4.7 Magnetic hyperthermia

The magnetic hyperthermia experiment was carried out to examine the heating rate of the ferrofluid using the Magnetherm unit (nanoTherics, U. K.). The experiments were performed in a microcentrifuge tube with 2 mL of ferrofluid. The heating rate for the ferrofluids was noted down from 30 to 60 °C with the help of an optical fiber temperature probe (~ error ±0.1 °C). The heating efficiency of the magnetic material was defined by the terms specific loss power (SLP) and ILP, which can be calculated by the equations given earlier chapter 1 (Equations 1.3 and 1.4).

2.4.8 *In-vitro* studies

The *in-vitro* cytotoxicity study of the ferrofluid was carried out with A549 cells using SRB assay. The cells were obtained from National Centre for Cell Sciences, Pune (India). The A549 cells were grown in DMEM (Dulbecco's Modified Eagle Medium) supplemented with 10% v/v fetal bovine serum, kanamycin (0.1 mg/mL), penicillin G (100 µg/mL), and sodium bicarbonate (1.5 mg/mL) at 37 °C in a 5% CO_2 atmosphere.

The volume of 100 µL of A549 cell suspension in media was added into the wells of a 96 well plate (5000 cells/well) and incubated at 37° C and 5 % CO_2 for 24 h. After incubation for 24 h, the old media was replaced by a new one. The different concentrations of the sterile MNPs or ferrofluid were added with concentrations of 0.1, 0.5, 1, 1.5, 2, 2.5, and 3 mg/mL. It was followed by incubation of the treated cells for 24 and 48 h. After 24 h, one plate was terminated by the addition of 50 µL cold aqueous TCA (80%) and kept at 4 ºC for 1 h to fix the cells. After that, the plates were washed several times with deionized water gently and allowed to dry at room temperature. Then, 50 µL of 0.4 % wt./v of SRB solution in 1% acetic acid was added to each well and kept at room temperature for 1 h. The unattached SRB was removed from the well by 1 % v/v acetic acid. It was followed by the addition of 100 µL of 10 mM Tris base solution (pH~ 10.5) to each well. Finally, the absorbance was taken at 510 nm. Similarly, the experiments were repeated for the cells treated with MNP_S after 48 h of incubation. Each experiment was carried out in triplicate. The % cell viability was estimated w.r.t. control untreated cells i.e. cells without nanoparticles by the equation [148]:

$$\% \text{ cell viability} = \frac{\text{Absorbance tested}}{\text{Absorbance control}} \times 100 \quad \ldots\ldots\ldots\ldots\ldots\ldots\ldots\ldots 2.2$$

In addition, a fluorescence microscope was used to record the image of the cells treated with MNP_S to observe the effect. Initially, 5000 cells/well were seeded with 100 µL of media (DMEM) into the 96 wells plate and incubated inside the CO_2 incubator for 24 h. After that, the consumed media was replaced by a fresh media and ferrofluid of known concentration (1 mg/mL). The culture plate was incubated further for 48 h. This was followed by washing the cells twice by PBS solution. Then the cells were stained with acridine orange (100 µg/mL) to determine the lysosomal vacuolation, autophagy, and apoptosis of the cells.

2.4.9 Experimental details for the photocatalytic

A) Catalytic degradation of p-nitrophenol

The oxidative catalytic degradation of PNP was investigated using the nanocomposites (*viz.* Fe_3C/C, $Fe_3C/Fe_3O_4/C$ and Ni-(Fe_3C/Fe_3O_4)/C). For this, 100 µL catalyst (1 mg/mL DW) suspension was mixed with 2 mL of PNP (0.2 mL of 7.2×10^{-7} M diluted with 2 mL DW) solution at pH 3. The pH of the PNP was maintained with the help of 0.1 M HCl and 0.1 M NaOH solution. Then, the suspension was held (1 h) for the adsorption till its equilibrium. Furthermore, the 30 µL of 2 M H_2O_2 (Merck) solution was added into the suspension then kept in the absence of any light and under visible light (cool white LED, ~94 mW/cm^2). The reactions were conducted in both media to compare the Fenton and photo-Fenton activities of these nanocomposites.

B) Catalytic degradation of methyl orange over S1 and S2

The catalytic degradation of MO was observed in the presence of different nanocomposites (e.g. Fe_3C/C, $Fe_3C/Fe_3O_4/C$ and Ni-(Fe_3C/Fe_3O_4)/C). For this, 100 µL of the dispersed catalyst (1 mg/mL, DW) was added into 2 mL of the MO solution (0.1 mL of 4.58 x 10^{-7} M diluted with 2 mL DW) at pH 3. This suspension was kept

for adsorption (1 h) until equilibrium was achieved. Further, 30 µL of 2 M H_2O_2 solution was added to the reaction mixture and put it into the absence of light and visible light for the comparison of the behavior of Fenton and photo Fenton activities.

2.4.10 Electrode assembly and electrochemical test

The electrochemical performance of the samples was evaluated against the Li reference electrode. To prepare the working electrodes of the present materials, the powders were mixed with carbon black and PVDF in 8:1:1 weight ratio. The slurry (prepared using N-Methyl-2- pyrrolidone, NMP) was coated on copper foil and dried at 100 ℃ until the solvent got evaporated completely. The electrochemical performance of each obtained product was evaluated with a 2032 coin-type cell using a non-aqueous electrolyte (1 M $LiPF_6$/EC: DMC = 1:1 in volume) and a polypropylene separator (Celgard 3501) against lithium metal. The cells were assembled in a glovebox filled with high purity argon. Electrochemical cycling was performed within the voltage range of 0.01–3 V (*vs.* Li/Li^+). The current *vs.* voltage variations (CVs) were measured in the potential range of 0.01-3 V (*vs.* Li/Li^+) at the scan rate of 0.1 mV s^{-1} at 25 ℃.